JOURNAL OF MATERIALS SCIENCE 14 (1979) 275–286

Temperature dependence of the flow stress and ductility of annealed and unannealed amorphous $Fe_{40}Ni_{40}P_{14}B_6$

D. J. KRENITSKY, D. G. AST
Department of Materials Science and Engineering, Cornell University, Ithaca, New York 14853, USA

The flow stress and ductility of amorphous $Fe_{40}Ni_{40}P_{14}B_6$ was investigated on as-prepared and annealed ribbons over the temperature range 78 to 573 K. The embrittlement is characterized by a rise in the ductile-to-brittle transition temperature T_{dtb}, such that $T_{dtb} \approx T_{anneal}$ and sets in at temperatures as low as 423 K. The flow stress of $Fe_{40}Ni_{40}P_{14}B_6$ at room temperature is 2.21 GPa (320 ksi), in good agreement with the extrapolation from hardness measurements. The flow stress increases with decreasing temperature. The increase can be accounted for in dislocation-based models of the deformation of a metallic glass but is more difficult to understand in terms of a free volume model.

1. Introduction

Knowledge of the temperature dependence of the flow stress, σ_y, of Fe-base metallic glasses is of interest in the development of deformation models for these materials. Unfortunately, no direct measurements are available, since these metallic glasses can only be prepared in the form of thin ribbons which fracture in a macroscopically brittle fashion when tested in tension. The fracture strength, σ_f, of a brittle material is not necessarily identical to σ_y, because failure may be controlled by the stress necessary to propagate existing defects, such as cracks, rather than being determined by the intrinsic properties of the material. The fracture strength of $Fe_{40}Ni_{40}P_{14}B_6$, even if measured on carefully prepared specimens with

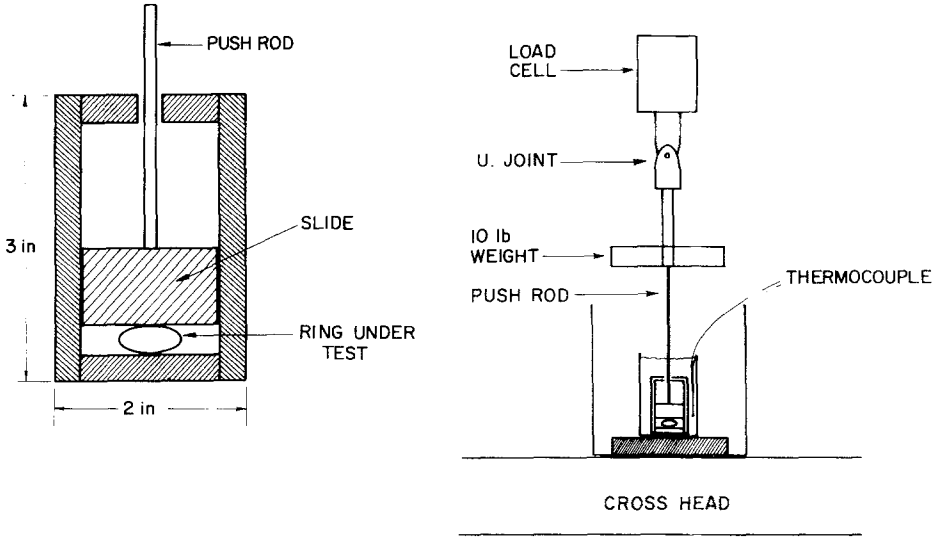

Figure 1 Experimental arrangement used for measuring flow stress as a function of temperature.

© 1979 Chapman and Hall Ltd. Printed in Great Britain.

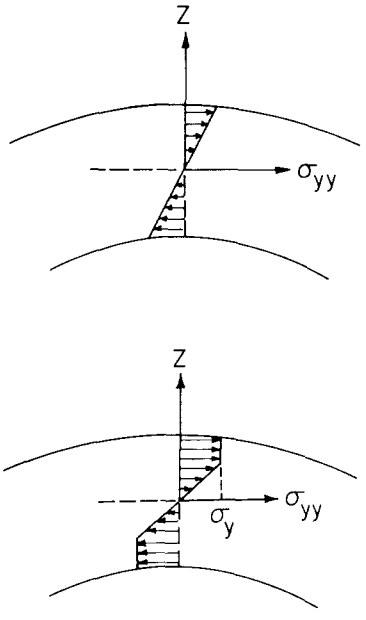

Figure 2 Stress distribution in the ribbon for the elastic (a) and mixed elastic–plastic case (b).

reduced cross-sections, consistently lies below the value expected from hardness measurements, which indicates that in this alloy $\sigma_f < \sigma_y$ [1].

This paper presents a technique for measuring the flow stress of metallic glasses which avoids the instability problems of the tensile test. The result obtained for the room temperature flow stress is in good agreement with the prediction from hardness measurements. The flow stress increases with decreasing temperature, and at 78 K is about 25% higher than at room temperature.

2. Principle of measurement

The flow stress is measured by coiling the ribbon into a ring which is then compressed between two parallel platens (see Fig. 1).

At the initial stage of the compression, the deformation is entirely elastic and the longitudinal stress, σ_{yy}, is a linear function of the distance z from the neutral axis (see Fig. 2a). When σ_{yy} reaches σ_y, plastic deformation begins at the surface of the ribbon in the form of densely spaced shear bands which, upon further deformation, spread towards the interior. The deformation is self-arresting, i.e., stable, even in the absence of work-hardening, since the shear bands cannot proceed past the neutral axis. Because of the absence of work-hardening in metallic glasses [2], the shear bands fix the stress level at σ_y and the stress level in the material closely approximates to that of an ideal elastic–plastic solid (Fig. 2b). In order to extract σ_y from the compression test, one needs to know how the tensile test variables, i.e., the force F applied to the platens and the distance between the platens, are related to the bending parameters, i.e., the local radius R at the apex, and l, the length of the lever arm with which the restoring moment M acts on the platens. In the elastic range, the relationship between R, l and ξ can be found using the theory of elastica [3]. Since we are also interested in the mixed elastic–plastic case, the relation was experimentally determined (see Fig. 3). Over the range of interest, the relation can, to a satisfactory approximation, be represented by a linear relation. This leads to the following simple predictions for the relationship between the force on the platens and the platen separation.

(a) Elastic range:

$$F = \frac{2wEd^2K}{3(1-\nu^2)\xi^2} \tag{1}$$

(b) Mixed elastic–plastic range:

$$F\xi = \frac{\sigma_y d^2 w}{2(0.653)(1-\nu^2)} - \frac{2(0.422)^2 K w \sigma_y{}^3 \xi^2}{3(0.653)E^2(1-\nu^2)}$$

$$K = 1-\nu^2+\nu\sqrt{[(1-\nu^2)/3]} \tag{2}$$

where E is Young's modulus, d the thickness of the ribbon, w the ribbon width, and ν Poisson's ratio and ξ the platen separation. Equations 1 and 2 predict a linear relation between F and $1/\xi^2$ in the elastic range and between $F\xi$ and ξ^2 in the mixed elastic–plastic case. If E and ν are known the slope of F versus $1/\xi^2$ of the elastic solution can be used to determine d, the effective ribbon thickness. This quantity varies somewhat along the ribbon and is, because of the uneven surface, not easily determined otherwise. The flow stress, σ_y, can then be found by either noting the onset of deviation from the predicted linear elastic behaviour, or from the intercept or the slope of the mixed elastic–plastic behaviour. (The latter two determinations are independent of each other, and experimental agreement between the two is a sensitive test of whether or not the assumption of an ideal elastic–plastic solid can be applied to the material under investigation.)

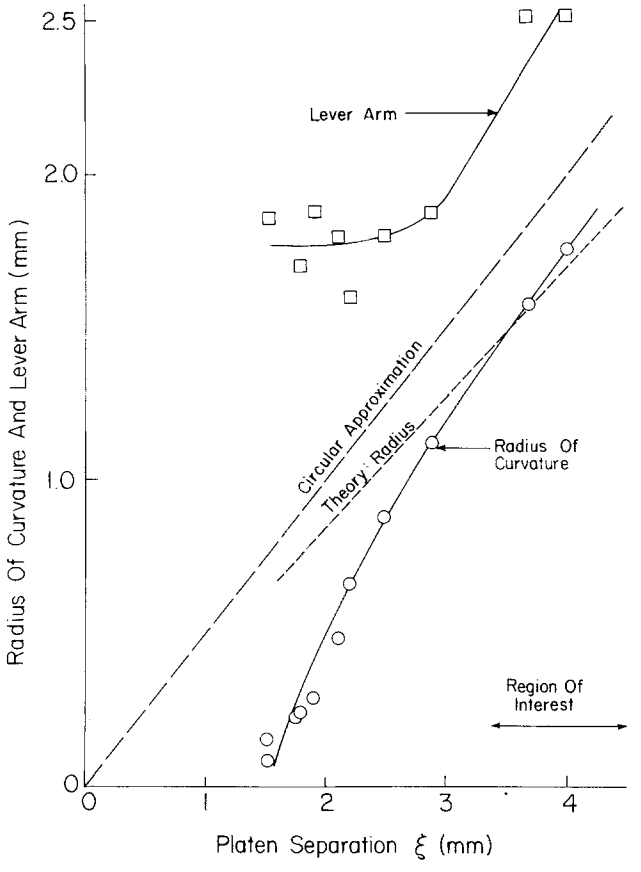

Figure 3 Relation between platen separation and radius of curvature at apex of ribbon under test.

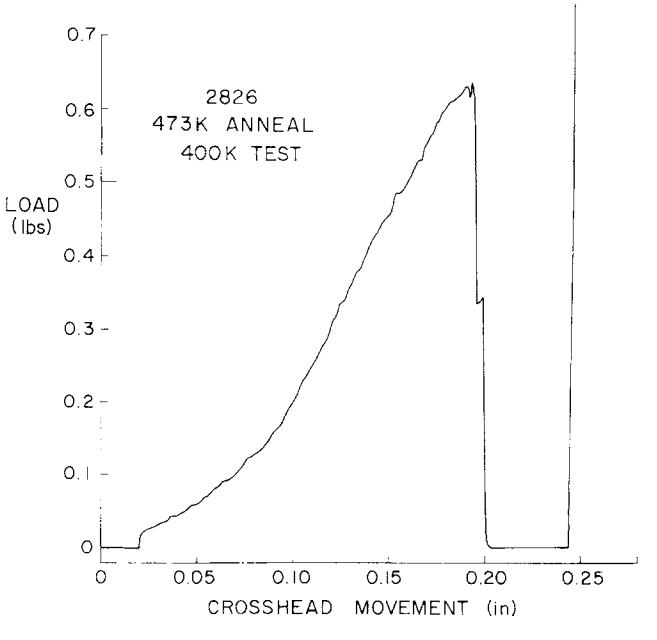

Figure 4 Load on platen versus platen separation for a specimen annealed at 473 K and tested at 400 K.

3. Experimental arrangements

The material was obtained from Allied Chemical (Trade name Metglas 2826) in the form of a continuous thin ribbon of ~ 2 mm width and 0.05 mm thickness. For compression tests, the material was coiled into single loops of 1 cm diameter, which were spot-welded. Annealing treatments were carried out, for a period of 1 hour, in a vacuum furnace with a base pressure of $\sim 1.3 \times 10^{-2}$ Pa ($\sim 10^{-5}$ Torr).

The rings were loaded into a parallel platen test arrangement fabricated of Cu, which is depicted schematically in Fig. 1. This apparatus was lowered into a stainless steel and brass dewar arrangement filled with a suitable temperature bath (LN_2, *n*-pentane, silicone oil) and inserted into an Instron testing machine. Compression of the platens was carried out at a cross-head speed of 0.508 cm min^{-1}. The corresponding maximum strain rates in the ribbon are $\sim 2 \times 10^{-2}$ sec^{-1} for $1/\xi = 3$ cm^{-1} and ~ 2 sec^{-1} for $1/\xi = 30$ cm^{-1}. Data analysis according to Equation 1 and 2 was carried out by replotting the data with the help of a Data General Nova equipped with a Tektronix graphic copy terminal. Slopes and intercepts were determined by a least squares fit over the linear parts of the plot.

4. Results

A typical result of a run is shown in Fig. 4. As the ring is increasingly compressed the load increases rapidly until first one side of the ring breaks, followed by the other, causing a step-like fall off. Eventually, the top platen contacts the bottom, and the load increases rapidly. The onset of this increase, corrected for the ribbon thickness, gives the position of zero platen serparation.

The platen separation at which fracture occurs is a qualitative measure of the ductility of the material and was therefore investigated in some detail.

Fig. 5 to 9 show the inverse platen separation at failure versus test temperature for both as-received material and material annealed at 423, 473, 523 and 573 K. Fig. 10 summarizes the results. It can be seen that annealing treatments as low as 423 K have a pronounced influence on the ductility of the material. The embrittlement disappears rapidly when the test temperature exceeds the annealing temperature.

In unannealed samples, the ductility decreases noticeably with decreasing temperature. Annealing, by sharply lowering the ductility at higher temperature, reduces the temperature dependence of the ductility.

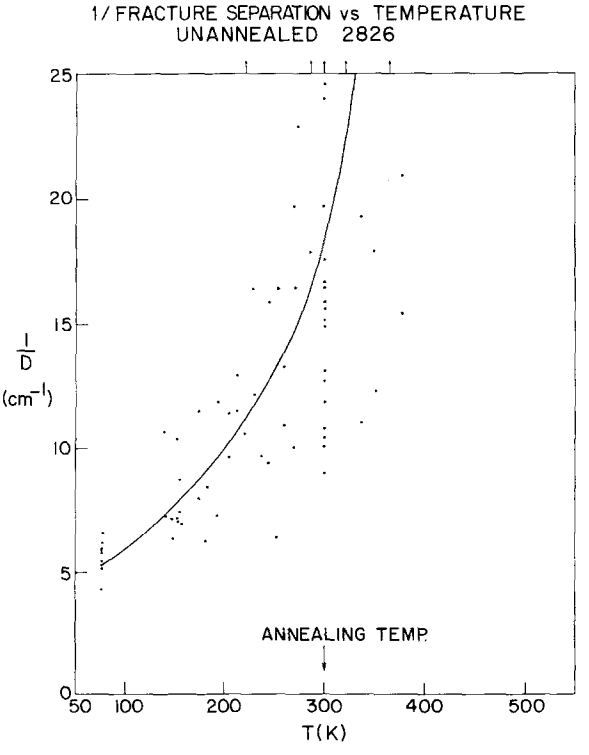

Figure 5 Reciprocal fracture separation versus temperature for unannealed $Fe_{40}Ni_{40}P_{14}B_6$.

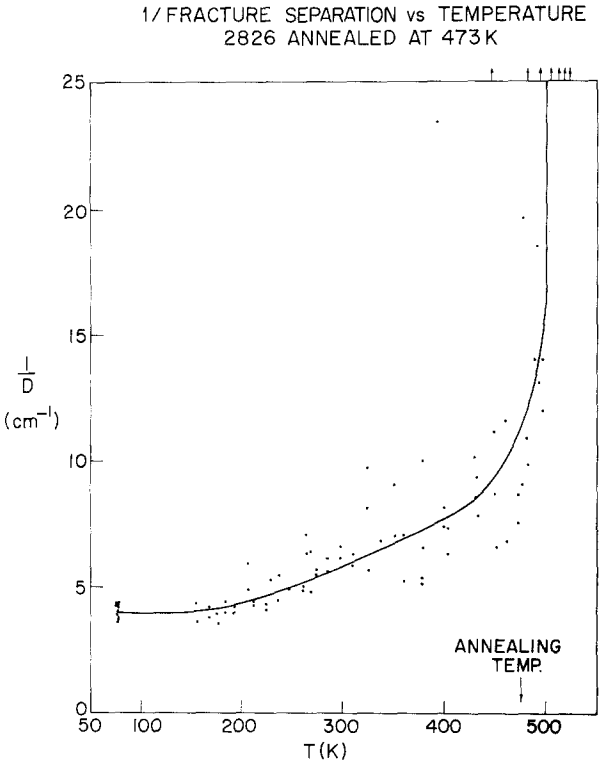

Figure 6 Reciprocal fracture separation versus temperature for $Fe_{40}Ni_{40}P_{14}B_6$ annealed at 423 K.

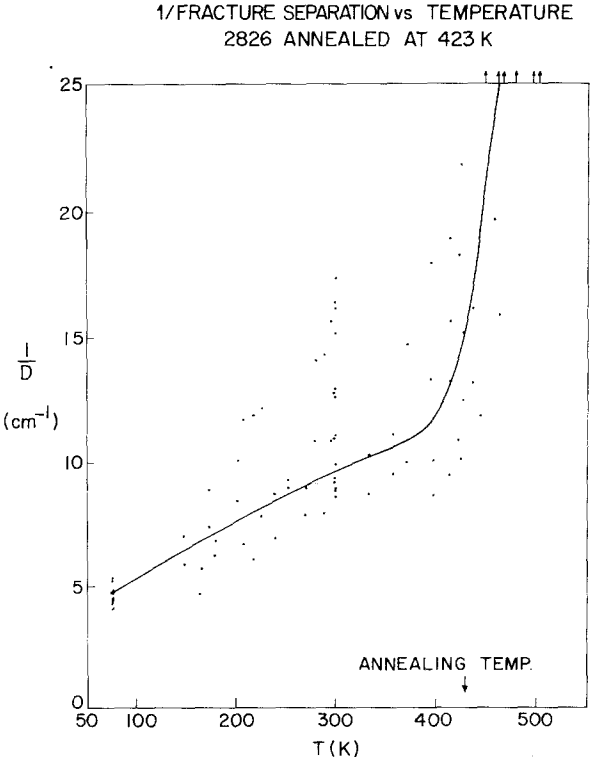

Figure 7 Reciprocal fracture separation versus temperature for $Fe_{40}Ni_{40}P_{14}B_6$ annealed at 473 K.

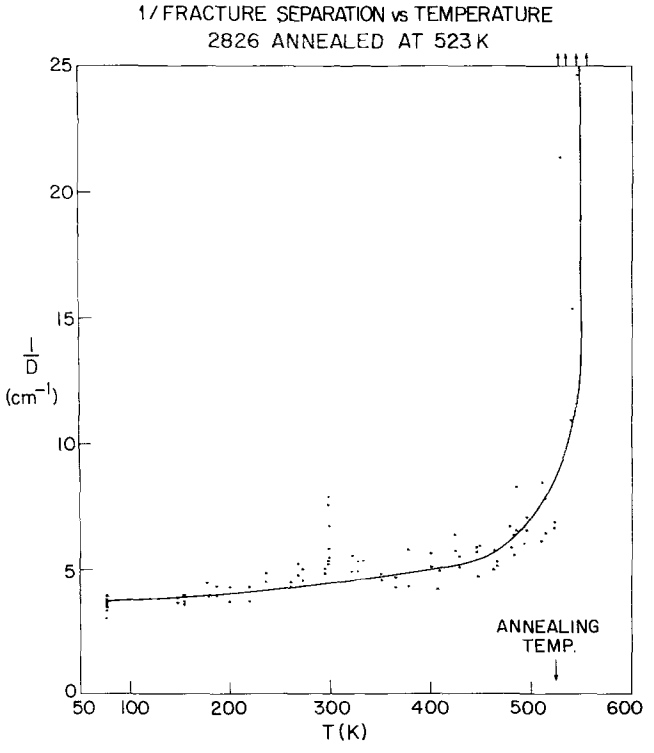

Figure 8 Reciprocal fracture separation versus temperature for $Fe_{40}Ni_{40}P_{14}B_6$ annealed at 523 K.

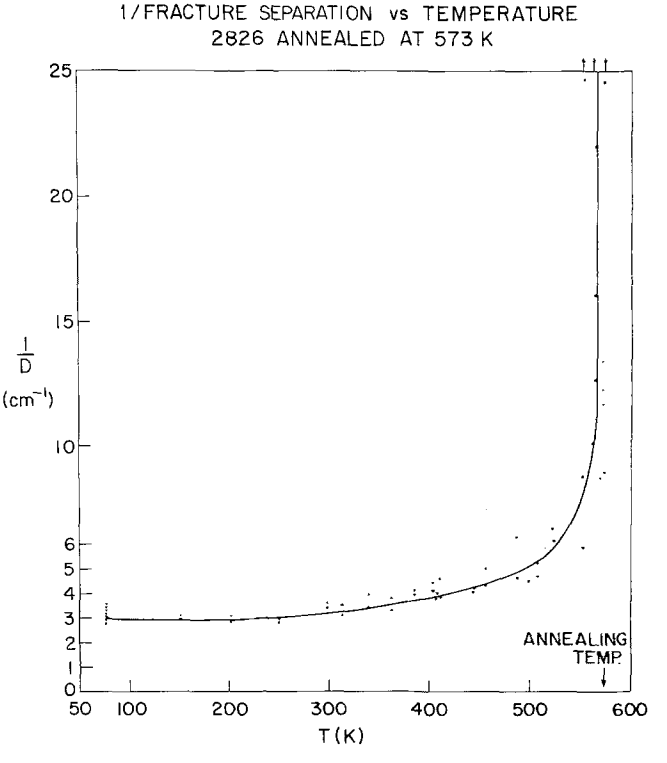

Figure 9 Reciprocal fracture separation versus temperature for $Fe_{40}Ni_{40}P_{14}B_6$ annealed at 573 K.

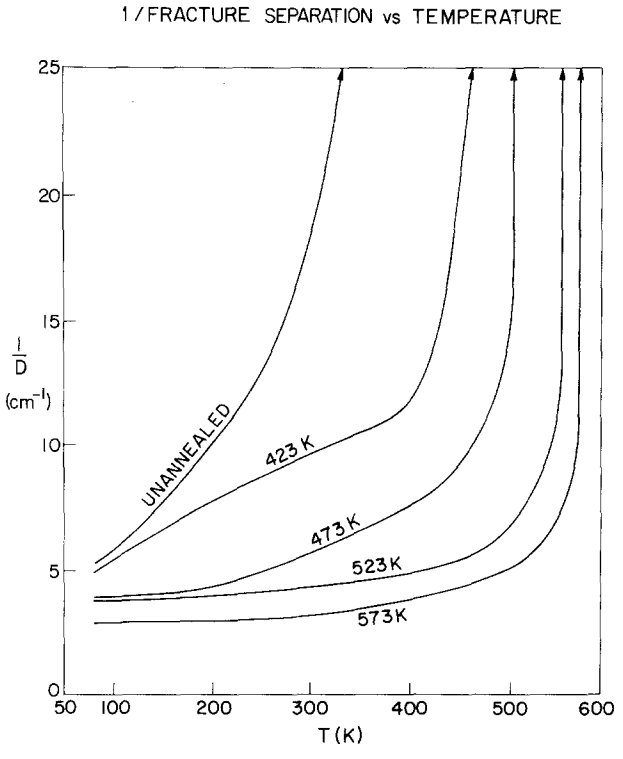

Figure 10 Summarized results for the influence of annealing on inverse fracture separation of amorphous $Fe_{40}Ni_{40}P_{14}B_6$.

In order to extract the flow stress, the deformation data were replotted as indicated by Equations 1 and 2. The results for the data of Fig. 4 are shown in Figs. 11 and 12. From Fig. 11 it can be seen that deviation from the elastic solution occurs very gradually, which makes it difficult to determine σ_y reliability in this way. We therefore chose to determine σ_y from a least squares fit of the straight portion of the elastic–plastic plot (Fig. 12). The deviations from the straight line at large values of ξ^2 are caused by elastic behaviour. At small values of ξ^2 the deviations are due to "kinking" of the ribbon. In general, σ_y values determined from the intercept agreed within 10% with σ_y values determined from the slope. Since the intercept method contains d^2, we consider the slope method somewhat more reliable and all values reported here

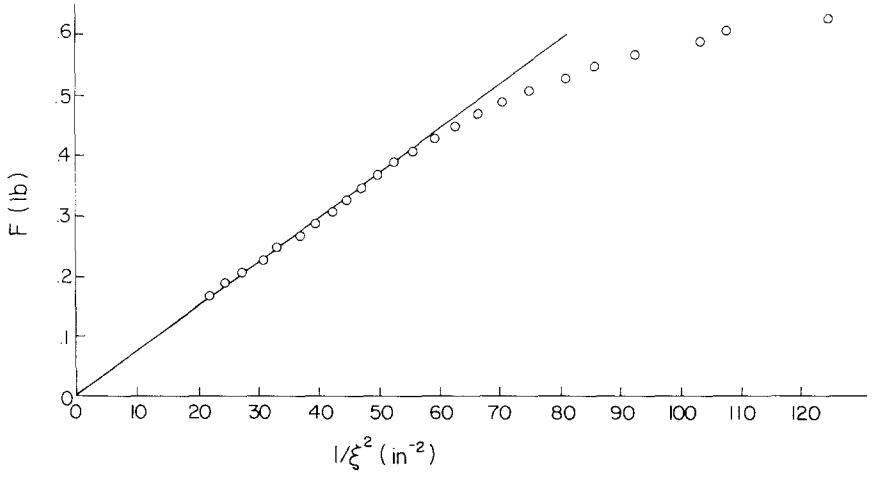

Figure 11 Force on platen (F) versus square of inverse platen separation ($1/\xi^2$) for a specimen annealed at 473 K and tested at 400 K (data of Fig. 4).

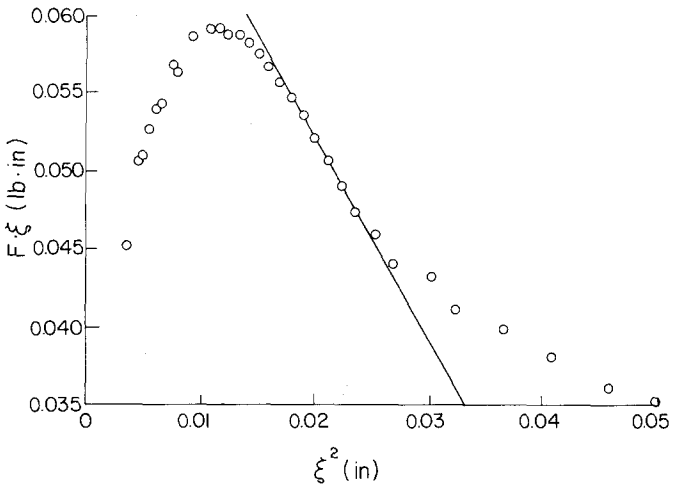

Figure 12 Force on platen separation versus squared platen separation for a specimen annealed at 473 K and tested at 400 K. (Data of Fig. 4).

were derived in this manner. The values for E and ν used in the analysis were 145 GPa (21 Mpsi) and 0.4.

For both as-received material and material annealed at 423, 473, 523 and 573 K, σ_y was determined as a function of temperature. The results of these measurements are depicted in Figs. 13 to 17. Fig. 18 summarizes the results. It can be seen that both unannealed and mildly annealed material exhibit a pronounced increase in flow stress at low temperature. At 78 K, the flow stress exceeds σ_y(RT) by about one quarter. This increase is not observed in heavily annealed material due to difficulties in obtaining a measurable long region of plastic behaviour. In this case it is difficult to determine reliably the slope of $F\xi$ versus ξ^2. From Fig. 12 it can be seen that any inadvertent inclusion of the elastic portion lowers the slope and thus the flow stress. For this reason we believe that the absence of a pronounced increase at low temperatures in heavily annealed material reflects experimental difficulties, rather than a real effect. The apparent increase in σ_y at temperatures near the annealing temperature is also an artifact and is caused by the onset of homogeneous relaxation.

5. Discussion

5.1. Ductility

Examination of the specimens shows that shear bands are formed at all test temperatures, in unannealed as well as in annealed specimens

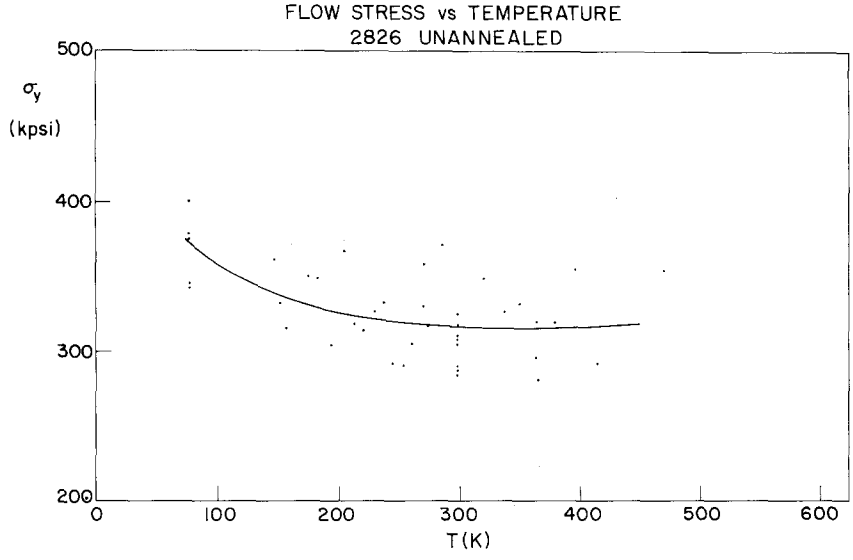

Figure 13 Flow stress versus temperature for unannealed $Fe_{40}Ni_{40}P_{14}B_6$.

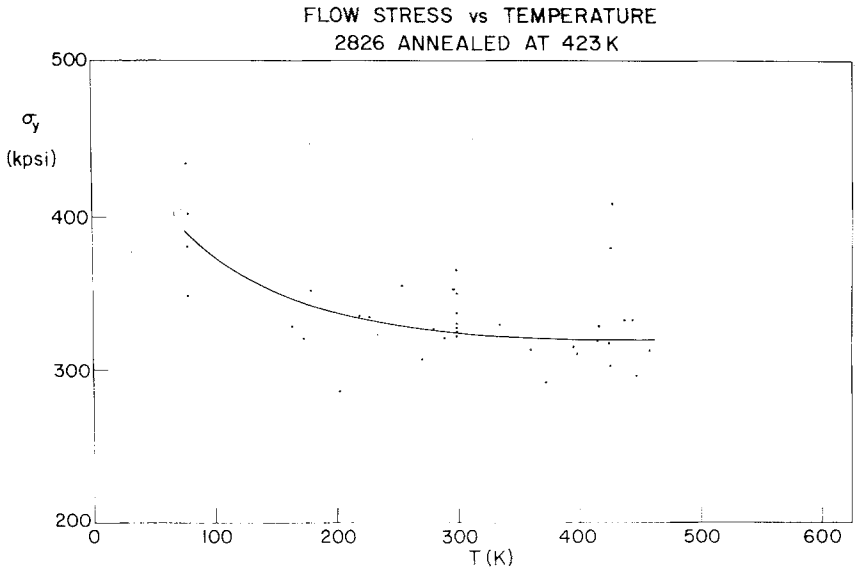

Figure 14 Flow stress versus temperature for $Fe_{40}Ni_{40}P_{14}B_6$ annealed at 423 K.

(Fig. 19). In addition to this inhomogeneous deformation process, a homogeneous deformation process also occurs. The contribution of the latter to the overall deformation is very small except if the test temperature is close to, or above the annealing temperature. In this case, homogeneous relaxation occurs at times comparable to the time scale of the experiment. The homogeneous process has been studied in more detail and will not be discussed here [4]. There are indications that the rapid increase in ductility at $T_{test} \approx T_{anneal}$ may not be solely due to homogeneous relaxation.

This evidence comes from conventional tensile tests on straight specimens which were pulled in an Instron testing machine equipped with a furnace. Prior to testing the specimens were annealed *in situ* for ten hours at selected temperatures between 423 and 573 K. These anneals were carried out under small loads in order to maintain specimen alignment. Such annealing results in specimens that shatter into many fragments when

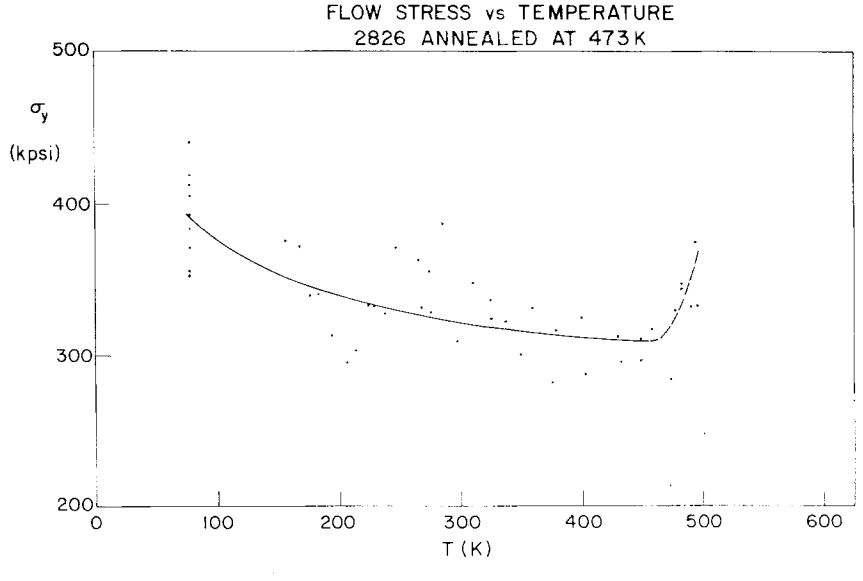

Figure 15 Flow stress versus temperature for $Fe_{40}Ni_{40}P_{14}B_6$ annealed at 473 K.

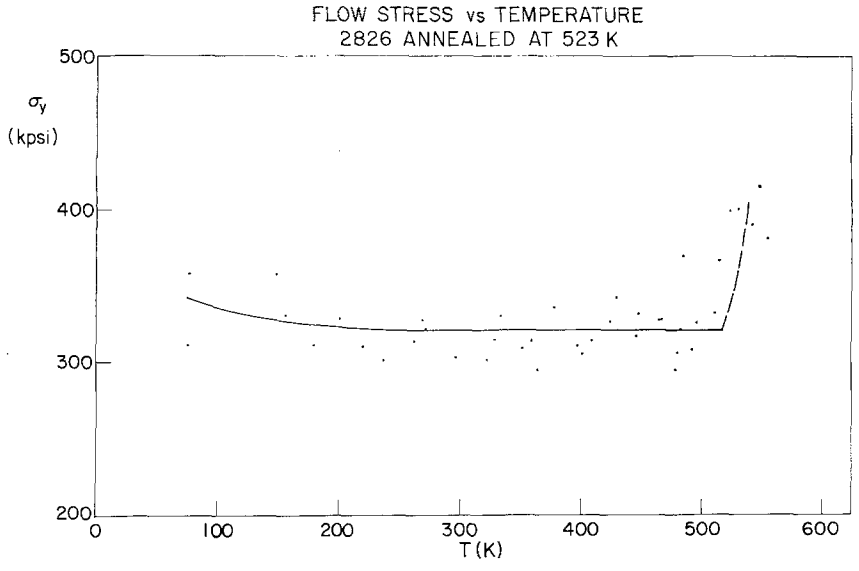

Figure 16 Flow stress versus temperature for $Fe_{40}Ni_{40}P_{14}B_6$ annealed at 523 K.

tested below the annealing temperature. However, when the annealed specimens are tested without lowering the temperature, these fail in the same manner as unannealed specimens tested at room temperature. That is, the specimens fracture at one point and the elastic recoil deforms the specimens (when viewed edge on) into an accordian-like shape. This deformation results from the production of shear bands and occurs much too rapidly for any significant homogeneous deformation to take place.

At $T_{test} \approx T_{anneal}$ even so-called embrittled specimens are ductile in the usual sense. Phenomenologically, the effect of annealing can be described as a shift in T_{dtb} towards T_{anneal}. This shift is noticeable after anneals at temperatures as low as 423 K and corresponds to the onset of exothermic activity in DSC experiments and to the onset

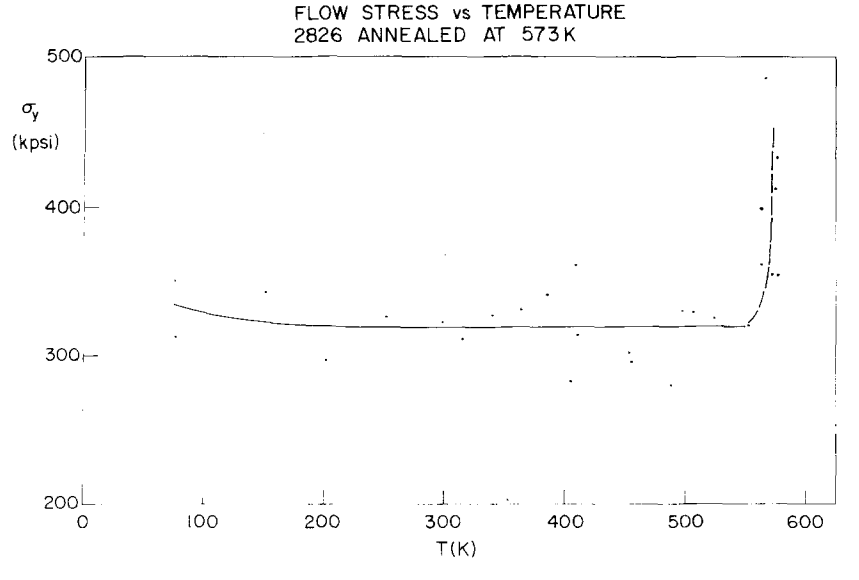

Figure 17 Flow stress versus temperature for $Fe_{40}Ni_{40}P_{14}B_6$ annealed at 573 K.

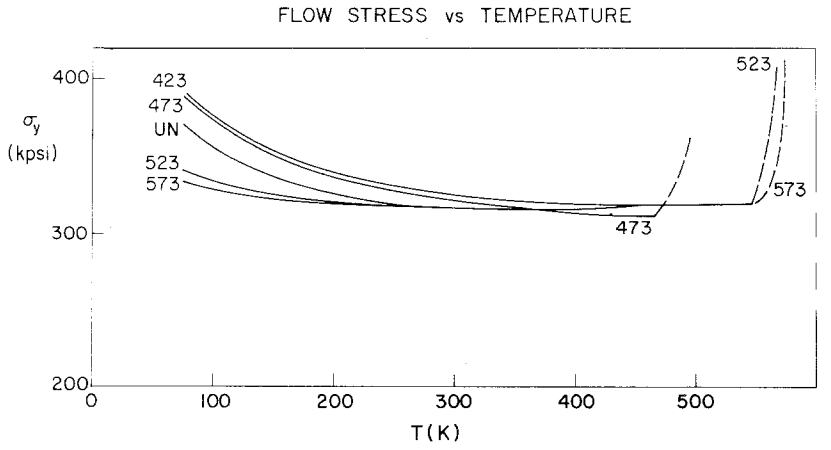

Figure 18 Summarized results for the influence of annealing on flow stress of amorphous $Fe_{40}Ni_{40}P_{14}B_6$

of clustering as observed in TEM studies of specimens first thinned and then annealed [5].

5.2. Flow stress

The room temperature flow stress of $Fe_{40}Ni_{40}P_{14}B_6$ determined in this investigation is 2.21 GPa (320 ksi) and, within the accuracy of the experiment, not influenced by annealing. The above value for σ_y is considerably higher than the reported yield stress by the manufacturer of 1.72 GPa (250 ksi) [6], and higher than the highest yield strength of 2.07 GPa (300 ksi) which we were able to measure in tension on a series of test specimens with reduced cross-sections and polished edges. The value of σ_y reported here, is in reasonable agreement with the value of 2.29 GPa (332 ksi) estimated from hardness measurements [1]. We believe therefore that in most cases tensile failure of $Fe_{40}Ni_{40}P_{14}B_6$ is controlled by existing flaws and that the fracture strength does not represent the flow stress of the material.

The flow stress of amorphous $Fe_{40}Ni_{40}P_{14}B_6$ increases with decreasing temperature. The behaviour is similar to that observed in crystalline materials where it is usually ascribed to an increase in Peierls stress. Thus the observed increase in σ_y at low temperatures can easily be accomodated by any deformation model which uses the movement of dislocations [7, 8]. It is more difficult to incorporate the observed increase into the frame-

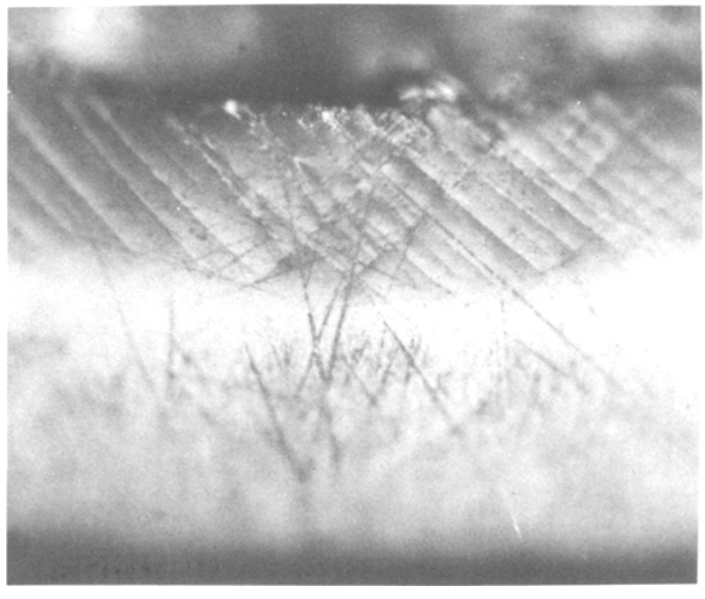

Figure 19 Shear bands formed by bending. The visibility of the bands has been enhanced by etching. The view is as in Fig. 2. The ribbon thickness (vertical dimension) is ~60 μm.

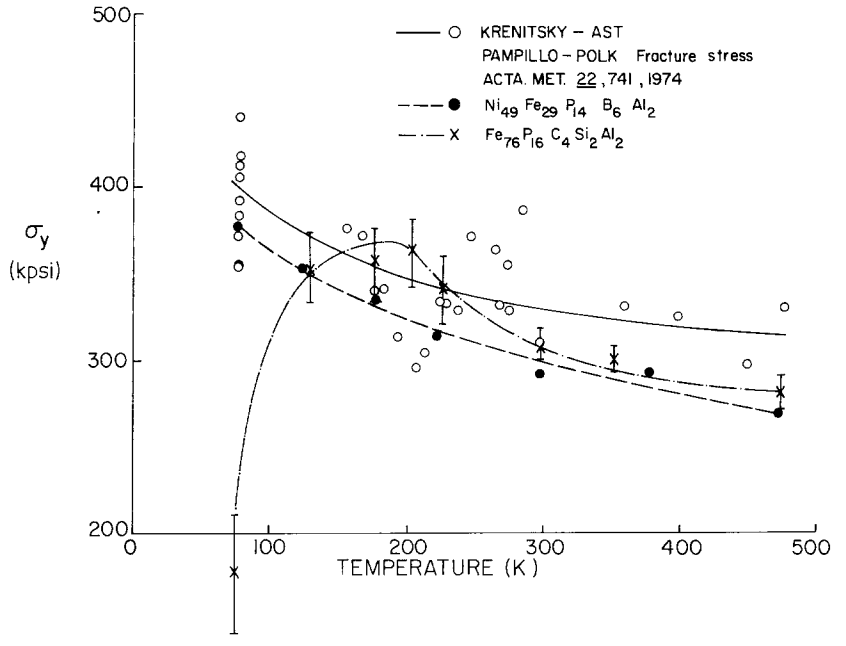

Figure 20 Comparison between the temperature dependence of the fracture strength of $Ni_{49}Fe_{29}P_{14}B_6Al_2$ and $Fe_{76}P_{16}C_4Si_2Al_2$ as reported by Pampillo and Polk and the temperature dependence of the flow stress of $Fe_{40}Ni_{40}P_{14}B_6$ as measured in this investigation.

work of free volume models which predict essentially a constant value of σ_y for temperatures below the glass transition temperature T_g [9] which in $Fe_{40}Ni_{40}P_{14}B_6$ is 643 K [5].

A comparable rise in fracture strength at low temperatures has been observed by Pampillo *et al.* [10] in Fe-based alloys of the composition $Ni_{49}Fe_{29}P_{14}B_6Al_2$ and $Fe_{76}P_{16}C_4Si_2Al_2$. These results, together with the flow stress reported here, are shown in Fig. 20. These authors have argued that the rise in fracture strength with decreasing temperature (except for $Fe_{76}P_{16}C_4Si_2Al_2$ below 200 K) reflects a rise of the flow stress. Our observations corroborate this claim.

6. Summary

The flow stress and ductility of as-received and of annealed amorphous $Fe_{40}Ni_{40}P_{14}B_6$ was investigated over the temperature range between 78 and 573 K by compressing loops of the material and assuming an ideal elastic–plastic behaviour in the analysis. It was found that the embrittlement sets in at temperatures as low as 423 K and is best described as a rise in the ductile-to-brittle transition temperature T_{dtb} such that $T_{dtb} \approx T_{anneal}$. The flow stress of $Fe_{40}Ni_{40}P_{16}B_6$ at RT is 2.21 GPa (320 ksi) in good agreement with hardness measurements. The flow stress increases with decreasing temperatures which is compatible with what one would expect from dislocation models for the deformation of metallic glasses.

Acknowledgements

This research was sponsored by the Office of Naval Research (NR039-151/N0014-77-C-0546) and the Materials Science Center at Cornell University.

References

1. L. E. TANNER and R. RAY, *Scripta Met.* **11** (1977) 783.
2. T. MASUMOTO and R. MADDIN, *Mater. Sci. and Engr.* **19** (1975) 1.
3. R. V. SOUTHWELL, "An Introduction to the Theory of Elasticity" (Dover Publications Inc., New York, 1969).
4. T. D. HADNAGY, D. J. KRENITSKY, D. G. AST and C. Y. LI, *Scripta Met.* **12** (1978) 45.
5. D. G. AST and D. J. KRENITSKY, *Mater. Sci. and Engr.* **23** (1976) 241.
6. Allied Chemical Preliminary Data Sheet.
7. J. C. M. LI, in "Frontiers in Materials Science", edited by L. E. Murr and C. Stein (Marcel Dekker, New York, 1976).
8. J. J. GILMAN, *J. Appl. Phys.* **46** (1975) 1625.
9. F. SPAEPEN and D. TURNBULL, *Scripta Met.* 8 (1974) 563.
10. C. A. PAMPILLO and D. F. POLK, *Acta Met.* **22** (1974) 741.

Received 8 February and accepted 19 May 1978.